Available online at www.sciencedirect.com
SCIENCE DIRECT®
Polymer 45 (2004) 949–960
polymer
www.elsevier.com/locate/polymer

Hyperbranched polymer/montmorillonite clay nanocomposites

Marlene Rodlert[a], Christopher J.G. Plummer[a], László Garamszegi[a], Yves Leterrier[a], Henri J.M. Grünbauer[b], Jan-Anders E. Månson[a,*]

[a]*Laboratoire de Technologie des Composites et Polymères (LTC), École Polytechnique Fédérale de Lausanne (EPFL), CH-1015 Lausanne, Switzerland*
[b]*Dow Benelux N.V., New Business Dev., NL-4530 AA Terneuzen, The Netherlands*

Received 28 October 2003; received in revised form 4 December 2003; accepted 5 December 2003

Abstract

Two to four pseudo-generation aliphatic hyperbranched polymers (HBPs) with –OH end-groups have been solution processed with various types of montmorillonite (MMT) layered alumino-silicate clays, and carefully dried to produce solid HBP/MMT nanocomposites. Exfoliated nanocomposites were obtained by processing the polyester HBPs with up to 20 wt% Na^+ MMT in water, and intercalation only became dominant at higher loadings, for which the MMT layer spacing was directly dependent on the HBP pseudo-generation number. Intercalation was observed at much lower MMT contents in HBPs processed with different organically modified MMTs in THF. In this case, the absolute MMT layer spacings in the nanocomposites showed little apparent dependence on the nature of the organic modifier and the pseudo-generation number of the HBP, although the difference between the final layer spacing and its value prior to mixing increased significantly with the polarity of the organic modifier. The various HBP/MMT nanocomposites were incorporated into polyurethane formulations by melt processing in the presence of a low molar mass polyol or solution processing in THF. Na^+MMT contents as low as 1.2 wt% led to an increase in the rubbery plateau modulus by about 60% with respect to that of the corresponding unfilled matrix, whereas much smaller relative increases were observed with unexfoliated or partly exfoliated MMT.

Keywords: Hyperbranched polymers; Nanocomposites; Thermoset

1. Introduction

Thermoset polymer/layered silicate clay nanocomposites may be referred to as either ‘exfoliated’ or ‘intercalated’ depending on whether the original stacked layer structure of the clay is maintained after processing with the polymer. The definition of exfoliation as loss in three-dimensional periodicity of the clay, which is consistent with common methods of characterization such as wide angle X-ray scattering (WAXS) or direct observation by transmission electron microscopy (TEM), will be assumed throughout in what follows. Such nanocomposites have been produced by a variety of processing routes, and in some cases, have shown marked improvements in physical and mechanical properties compared with those of the neat resin, particularly above the glass transition temperature, T_g [1–7]. Thus, significant increases in elongation at break, modulus and tensile strength have been reported in intercalated polyurethane elastomer nanocomposites containing various types of layered silicate [8–14]. This contrasts with the effect of conventional inorganic fillers, which are primarily employed to reduce cost and increase stiffness, but which generally reduce the strength and elongation to break [15,16]. Although thermoset nanocomposites are often prepared by swelling organically modified clays with a monomer precursor, it may be advantageous if intercalation and/or exfoliation can be achieved by combining suitably functionalized monomers or pre-polymers with a native layered silicate such as sodium montmorillonite (Na^+MMT). Aqueous solution processing of dendritic hyperbranched polyester polyols is of particular interest in this respect, because it offers a means of obtaining exfoliated clay nanocomposites from Na^+MMT without the aggregation associated with linear water soluble polyurethane precursors such as poly(ethylene glycol) (PEG) [17,18]. Hyperbranched polymers (HBPs) have a tree-like structure with a large number of branch points radiating from a multifunctional core molecule, and hence a potentially high degree of end-group functionality per molecule [19,20].

* Corresponding author. Tel.: +41-21-693-4281; fax: +41-21-693-5880.
E-mail address: jan-anders.manson@epfl.ch (J.-A.E. Månson).

0032-3861/$ - see front matter © 2003 Published by Elsevier Ltd.
doi:10.1016/j.polymer.2003.12.015

(The –OH end-groups are assumed to be concentrated in the periphery of the molecules in a hydrophilic environment.) Polyester HBPs also show excellent processing characteristics and shrinkage control, and are therefore promising in their own right for thermoset formulations [21–24].

The present study explores these possibilities by focusing on the morphology of nanocomposites obtained by solution processing unmodified Na^+MMT and organically modified MMT with a range of –OH terminated HBPs. The HBP structure consists of dendritic units (D) (both end-groups reacted), linear units (L) (one end-group reacted) and terminal units (T) (neither end-group reacted), and the degree of branching DB may then be defined, for example, as shown schematically in Fig. 1(b) [25,26]. Although perfect dendrimers with degree of branching (DB) = 1 (Fig. 1(a)) may be of interest as model systems in this context because of their precisely defined structure, HBPs are less expensive to produce and are therefore of greater relevance to bulk applications, such as structural thermosets. To evaluate this potential, nanocomposites based on a commercial HBP have been incorporated into model polyurethane formulations, whose mechanical properties are also briefly discussed.

2. Experimental

2.1. Materials

2.1.1. Clays

Na^+MMT (cation exchange capacity (CEC) = 92 mequiv./100 g clay; 50% of particles <6 μm (maximum dimension); reported basal plane spacing, d_{001} = 1.17 nm) and a range of MMTs modified with quaternary ammonium salts were obtained from Southern Clay Products, dried and stored under vacuum prior to use. The modified MMTs referred to in what follows are Cloisite® 15A (dimethyl dihydrogenated tallow quaternary ammonium-MMT, 125 mequiv./100 g clay, 50% of particles <6 μm, d_{001} = 3.15 nm), Cloisite® 20A (dimethyl dehydrogenated tallow quaternary ammonium-MMT, 95 mequiv./100 g clay, 50% of particles <6 μm, d_{001} = 2.42 nm), Cloisite® 10A (dimethyl benzyl hydrogenated tallow quaternary ammonium-MMT, 125 mequiv./100 g clay, 50% of particles <6 μm, d_{001} = 1.92 nm) and Cloisite® 30B (methyl tallow bis-2-hydroxyethyl quaternary ammonium-MMT, 90 mequiv./100 g clay, 50% of particles <6 μm, d_{001} = 1.85 nm).

2.1.2. HBPs

Aliphatic polyester HBPs, prepared from 2,2-bis-(methylol)propionic acid (bis-MPA) and a tetrafunctional ethoxylated pentaerythritol (EPE) core (HBP-EPE), were supplied by Perstorp Chemicals. The use of a one-pot condensation, as opposed to stepwise synthesis, leads to a less regularly branched structure than the dendrimers. The different grades are therefore referred to by a pseudo-generation number, such that the *N*th pseudo-generation corresponds to a reaction mixture containing $f(1 + 2 + 2^2 + \cdots + 2^{N-1}$(bis-MPA molecules for every *f*-functional core molecule, that is, the same mean number of monomers per core as for the *N*th generation dendrimer analogue. A second series of HBP polyesters (HBP-TMP) was prepared in-house from bis-MPA and a trimethylolpropane (TMP) core, via a one-pot condensation at 140 °C with sulfuric acid as the catalyst [19]. To limit polydispersity, the bis-MPA was added to the reaction mixture steadily over a period of about 2 h. As shown in Table 1, the structural parameters of the HBP-TMP were similar to those of the HBP-EPE, although the 4 pseudo-generation HBP-TMP showed significantly greater polydispersity than the corresponding HBP-EPE, either because of inadequate control of the reaction conditions or

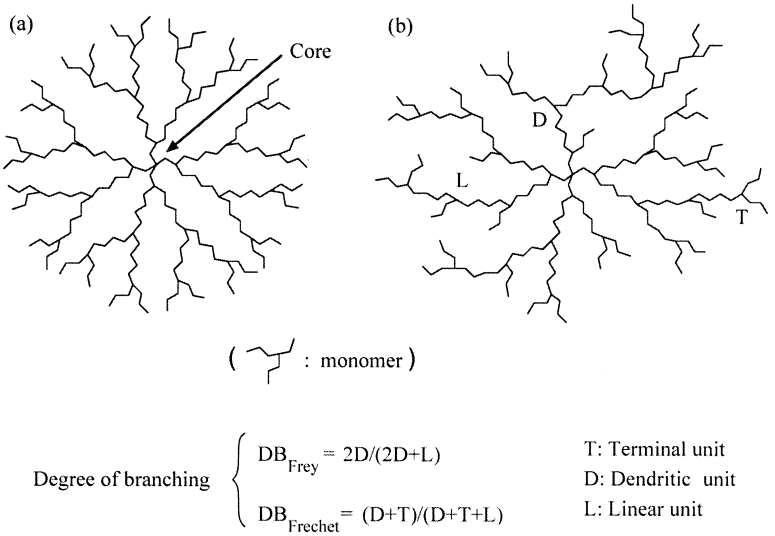

Fig. 1. Schematic structures of (a) a dendrimer and (b) a hyperbranched polymer, along with definitions of the degree of branching according to Frey and Frechet [25,26]; for the example shown in (b), DB_{Frey} = 67% and $DB_{Frechet}$ = 71%.

Table 1
Physical data for the hyperbranched polymers

Polymer	(Pseudo) generation	M_n[a] (g/mol)	M_n[b] (g/mol)	PD[b]	DB (Frey)	DB (Fréchet)	T_g (K)
HBP-EPE	2nd	1750	1130	2.1	0.3	0.43	281
HBP-EPE	3rd	3608	2520	2.9	0.31	0.42	296
HBP-EPE	4th	7323	4340	3.1	0.34	0.40	304
HBP-TMP	2nd	1179	1264	2.2	0.31	0.47	299
HBP-TMP	3rd	2573	2704	3.5	0.39	0.44	312
HBP-TMP	4th	5357	3006	7.5	0.40	0.42	327
Polyoxetane	–	–	2500	1.8	–	–	309

[a] Calculated from the stoichiometry.
[b] GPC data.

possibly because of increased steric hindrance to monomer addition to the more compact, less flexible TMP core. –OH-terminated aliphatic hyperbranched polyether (polyoxetane), synthesized by cationic ring-opening polymerization from 3-ethyl-3-(hydroxymethyl)oxetane [27], was kindly provided by the Royal Institute of Technology, Stockholm for comparison. Physical data for the different HBPs are given in Table 1 and representative structures are shown in Fig. 2.

2.1.3. Polyols and isocyanates

Poly(ethylene glycol) (PEG, $M = 300$ g/mol) and ethoxylated trimethylolpropane (ETMP, $M = 446$ g/mol) were obtained from Fluka and Perstorp Chemicals, respectively, and stored over a molecular sieve prior to use. Modified diphenylmethane diisocyanate (MDI, $M_w = 286$ g/mol) with a mean functionality of 2.2 was provided by Dow Europe.

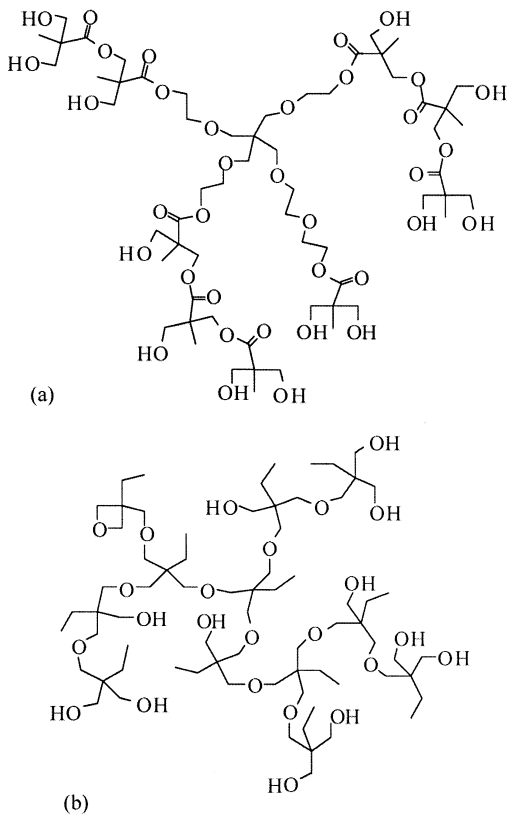

Fig. 2. Representative structures of (a) HBP-EPE and (b) polyoxetane.

2.2. Characterization

The structure of the HBPs was verified by gel permeation chromatography (GPC) and ^{1}H-NMR (600 MHz, Bruker AMX-600) in DMSO-d_6. ^{13}C-NMR was used to obtain the DB values in Table 1. Distinct peaks were assigned to dendritic units (D), terminal units (T) and linear units (L) [28]. The DB was then calculated from the corresponding peak areas, according to the definitions given in Fig. 1. GPC measurements were carried out in tetrahydrofuran (THF) using a Waters 150CV modified for on-line differential viscosimetry and universal calibration, as described in detail elsewhere [29]. For infra-red spectroscopy (FTIR), use was made of a Nicolet Magna DSP 650 FTIR spectrometer/Golden Gate ATR. Differential scanning calorimetry (DSC) was performed with a Perkin–Elmer DSC7 at a heating (or cooling) rate of 10 K/min on 10 mg specimens, using water and indium standards for calibration. WAXS spectra were recorded in reflection mode with a Siemens Kristalloflex 805 diffractometer at room temperature (Cu K_α radiation, $\lambda = 1.54$ Å; where necessary, the specimens were pressed between two glass plates at temperatures just above T_g, in order to obtain a flat surface). TEM observations were made using a Philips EM430 TEM operated at 300 kV under low dose conditions and at a magnification of about 40k ×, to minimize beam damage. Specimens of the different HBP/MMTs were embedded in epoxy resin, and 60 to 100 nm thick sections prepared with a Reichert Jung Ultracut-E microtome and a dry 45° diamond knife, and transferred to carbon coated copper grids. In the case of the polyurethanes, the sections were picked up from water. Rheological properties were investigated with a Rheometrics ARES (Advanced Rheometric Expansion System) rheometer in oscillating shear, with 8, 25 and 50 mm diameter parallel plates and a 0.3 to 0.6 mm gap. All rheological measurements were performed in the linear viscoelastic regime, whose extent was determined from constant frequency sweeps. Dynamic mechanical analysis (DMA) was carried

out in either tension or flexion using a Rheometrics Solids Analyzer (RSAII).

2.3. Nanocomposite preparation

HBP/Na^+MMT nanocomposites were prepared by dispersing the required amount of polymer, preheated to 150 °C to facilitate dissolution [30], and Na^+MMT in deionized water (10 wt% solids content) and mixing at about 100 °C in air using a magnetic stirrer. When the viscosity became too high to permit stirring, drying was continued at 60 °C under vacuum. Unless mentioned otherwise, THF was used as the solvent for nanocomposites prepared from the modified MMTs, in which case mixing was carried out at about 50 °C, again after preheating the HBP to 150 °C. As shown in Fig. 3 for the 2 pseudo-generation HBP-EPE/Na^+MMT, there were no major changes in the IR absorption peaks after processing, which was taken to imply minimal chemical alteration of the HBPs during the initial stages of sample preparation. The OH stretching band (centred on about 3300 cm^{-1}) is known to become narrower on heating, and the associated peak shifts to higher wavenumbers, effects that have been attributed to a decrease in hydrogen bonding [30].

Polyurethanes were prepared by either melt or solution processing. In the melt process, the required amount of HBP/MMT was preheated to 150 °C and mixed using a stirrer bar in a glass vessel with a liquid polyol (ETMP or low molar mass PEG) at 130 °C, to obtain a homogenous blend. The polyol blend and the MDI were then degassed under vacuum at room temperature, hand-mixed in stoichiometric amounts for a few seconds, poured into a metal mould and left to react for 5 h in an autoclave at 140 °C and 12×10^5 Pa. In the solution process, the HBP/MMT was preheated to 150 °C and dispersed in dry distilled THF at 50 °C. A stoichiometric amount of degassed MDI was added and the solution (30 wt% solids content) stirred for a further 15 min at 60 °C. It was then poured into an open steel mould, left to dry for 1 h at room temperature under dry N_2 and reacted for 12 h at 120 °C under vacuum. The specimens were post-cured for 1 h at 160 °C under vacuum to ensure complete reaction, taken to correspond to the disappearance of the NCO peak in the FTIR spectra.

3. Results and discussion

After drying and pressing, the HBP-EPE/Na^+MMT nanocomposite specimens (about 1 mm thick) obtained from dispersions in water were transparent for Na^+MMT contents of up to about 10 wt%, and although they were strongly birefringent, they did not contain discrete Na^+MMT particles large enough to be detectable by optical microscopy. At higher loadings, the specimens became yellowish and opaque. Their stiffness also increased markedly and it became difficult to prepare homogeneous specimens by compression moulding for Na^+MMT contents greater than 50 wt%. Fig. 4(a) gives WAXS spectra for 2 pseudo-generation HBP-EPE/Na^+MMT. The strong peak at $2\theta = 7.7°$ in the as-received Na^+MMT, which corresponds to a basal plane spacing $d_{001} = 1.15$ nm, moved to lower angles in the presence of the HBP, and it was no longer visible at Na^+MMT contents below 20 wt%. The same qualitative behavior was observed for 3 and 4 pseudo-generation HBP-EPE. However, as shown in Table 2, there was a systematic increase in d_{001} with pseudo-generation number at Na^+MMT loadings between 20 and 50 wt%,

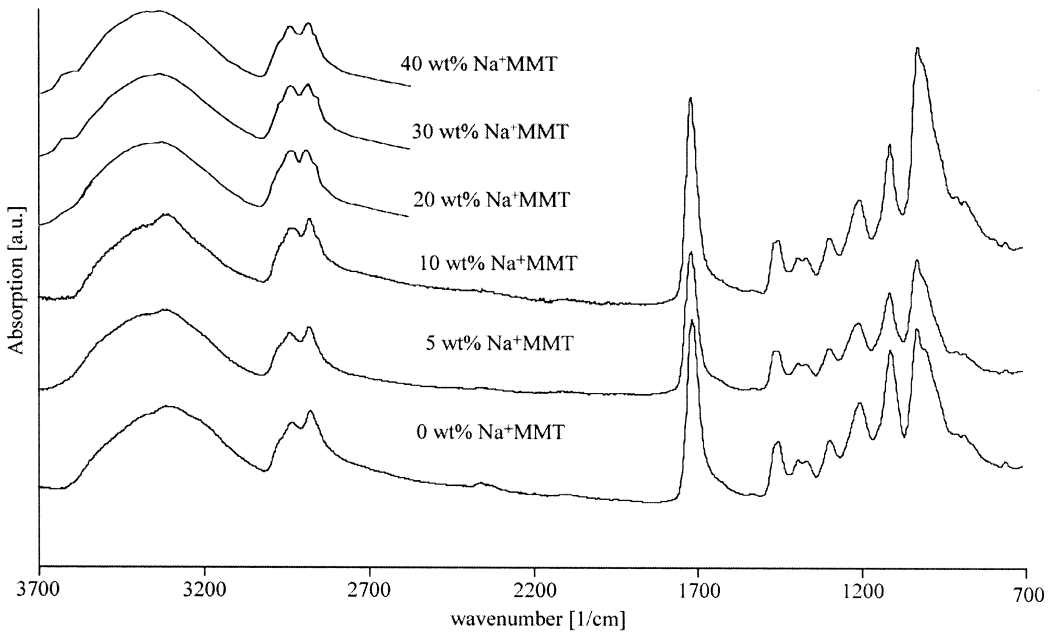

Fig. 3. ATR-FTIR spectra for 2 pseudo-generation HBP-EPE/Na^+MMT processed in water for the different Na^+MMT loadings indicated.

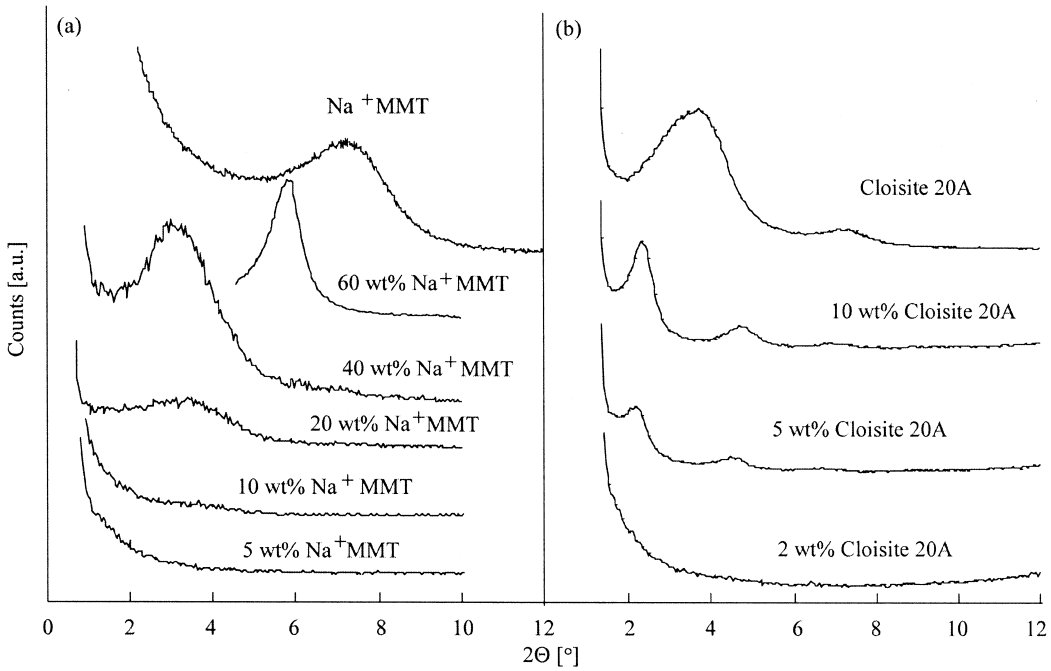

Fig. 4. WAXS spectra for (a) 2 pseudo-generation HBP-EPE/Na^+MMT processed in water and (b) 2 pseudo-generation HBP-EPE/Cloisite® 20A processed in THF, with different clay contents.

which will be discussed in more detail below. At higher Na^+MMT contents ($\geq$60 wt%), d_{001} decreased markedly.

Fig. 4(b) shows WAXS spectra for HBP-EPE/Cloisite® 20A prepared from THF. The organically modified MMT again underwent significant expansion. d_{001} increased from 2.4 nm to about 3.8 nm in the presence of 2 pseudo-generation HBP-EPE, for example. However, WAXS showed three-dimensional order to persist down to loadings of about 2 wt%, i.e. a silicate content of 1.24 wt%, bearing in mind that Cloisite® 20A contains about 38 wt% alkylammonium modifier. Moreover, the higher order reflections in the WAXS spectra indicated more coherent long-range order than for the intercalated Na^+MMT nanocomposites. Use of Cloisite® 15A and 30B also resulted in d_{001} close to 3.8 at 20 wt% clay, in spite of the marked differences in the initial values of d_{001} and polarity in the different clays. (Cloisite® 30B contains a relatively hydrophilic modifier whereas the tail groups of the Cloisite® 15A and 20A modifiers are hydrophobic.) On the other hand, data for the increase in d_{001} with respect to its initial

Table 2
The basal plane spacing, d_{001}, as a function of clay content for the different nanocomposites specified. The crosses refer to specimens in which no Bragg peaks were observed in the relevant range

Polymer (pseudo-)generation number/clay/solvent	d_{001} (nm) for different clay contents (wt%)										
	2	5	10	15	20	30	40	50	60	80	100
HBP-EPE 2/Na^+MMT/H_2O	×	×	×	×	2.5	2.8	2.7		1.5	1.5	1.2
HBP-EPE 3/Na^+MMT/H_2O	×	×	×	×	2.8	3.0	2.8		1.9	1.6	1.2
HBP-EPE 4/Na^+MMT/H_2O	×	×	×	×	3.7	3.9	3.6	3.5	2.1	1.5	1.2
HBP-EPE 2/Cloisite® 20A/THF	×	4.0	3.9		3.8		3.6		3.4		2.4
HBP-EPE 4/Cloisite® 20A/THF			4.0		3.7		3.7		3.3		2.4
HBP-EPE 2/Cloisite® 15A/THF			3.9		3.8		3.9		3.8		3.2
HBP-EPE 4/Cloisite® 15A/THF			3.9		3.9		3.7		3.9		3.2
HBP-EPE 2/Cloisite® 30B/THF			4.1		3.9		3.6		3.8		1.9
HBP-EPE 4/Cloisite® 30B/THF			3.9		3.7		3.4		3.8		1.9
HBP-EPE 2/Cloisite® 10A/THF			3.5		3.5		3.3		3.6		1.9
HBP-EPE 4/Cloisite® 10A/THF			3.7		3.5		3.4		3.3		1.9
HBP-TMP 2/Na^+MMT/H_2O	×	×	×	×	×		2.4				1.2
HBP-TMP 3/Na^+MMT/H_2O	×	×	×	×	×		2.9				1.2
HBP-TMP 4/Na^+MMT/H_2O	×	×	×	×	×		3.0				1.2
Polyoxetane/Cloisite® 20A/THF	3.7	3.7	3.5	3.6	3.6						2.4
Polyoxetane/Cloisite® 30B/THF		3.5	3.4		3.5						1.9

value (Fig. 5), showed Cloisite® 30B to undergo particularly strong expansion at low to intermediate clay contents, comparable with that observed in the 2 and 3 pseudo-generation HBP-EPE/Na^+MMT dispersed in water. Indeed, the layer expansion at fixed clay content may be inferred from the data in Table 2 to increase significantly with increasing hydrophilicity, that is, Cloisite® 15A (0.46–0.67 nm) < Cloisite® 20A (1.16–1.60) < Cloisite® 10A (1.43–1.53) < Cloisite® 30B (1.54–2.20) [31]. Fig. 5 also reflects the relative insensitivity of d_{001} in the nanocomposites containing organically modified clay to the HBP pseudo-generation number. The solid curves in Fig. 5 are the values calculated for a homogeneous composite with a uniform layer spacing assuming densities of 2.86, 1.98 and 1.66 g/cm^3 for Na^+MMT, Cloisite® 30B and Cloisite® 15A, respectively.

Fig. 6 shows representative TEM micrographs corresponding to the results in Fig. 4. There was little order in 2 pseudo-generation HBP-EPE/10 wt% Na^+MMT (Fig. 6(a)), but at 20 wt% Na^+MMT, the localized regions of stacking that gave rise to corresponding peak in Fig. 4(a) were visible, albeit limited to 5 to 6 layer tactoids (Fig. 6(b)). 2 pseudo-generation HBP-EPE/10 wt% Cloisite® 20A (Fig. 6(c)), showed more extensive stacking, with a well defined basal plane spacing consistent with the position of the corresponding first order Bragg peak in Fig. 4(b).

The results of processing HBP-TMP with Na^+MMT in water were similar to those described above for HBP-EPE, as shown in Fig. 7 for 2 pseudo-generation HBP-TMP/Na^+MMT. Substantial exfoliation was observed at compositions up to and including 20% Na^+MMT, and at higher clay contents, where intercalation dominated, there was again a strong correlation between d_{001} and the pseudo-generation number.

The –OH functional polyoxetane was insoluble in water. Polyoxetane/Cloisite® 20A processed in THF, nevertheless showed behavior comparable with that of the polyester HBPs, that is, an increase in d_{001} to about 3.6 nm, which corresponded to increases in the layer separation of about 1.2 (Fig. 8). Attempts to produce exfoliated nanocomposites with 5 wt% Na^+MMT by processing in methanol instead of water led to an increase in d_{001} to about 1.5 nm, that is an increase in the layer separation of about 0.35 nm, which indicated weak intercalation only. Indeed, d_{001} did not reach more than about 1.8 nm in any of the HBPs dispersed with Na^+MMT in methanol or THF (Fig. 8). Similarly, dispersions of the organically modified clay in water with HBP-EPE and HBP-TMP led to relatively small increase in the layer separation.

A key factor in the effectiveness of HBPs in stabilizing aqueous dispersions of Na^+MMT is thought to be their ability to bring high degrees of end-group functionality to an interface without the entropy penalties associated with high tethering densities of linear end-functionalized polymers of comparable molar mass. Moreover, an isolated linear polymer chain with functional groups distributed uniformly along its length will tend to collapse onto a substrate with which the functional groups interact strongly. An isolated Gaussian chain is predicted to be confined to a layer of thickness $h \approx 2a/\zeta$, at the substrate surface, where a is the statistical segment length and ζkT is the interaction energy per segment, so that for interactions of the order of kT, the chain will therefore effectively lie flat on the substrate. It was suggested previously that collapse of a dendritic polymer with relatively short branches onto a substrate should be sterically hindered [18]. However, simple molecular dynamics simulations have shown that such collapse is possible regardless of the generation number, even for the perfect polyester dendrimer analogues to the HBPs under consideration here, consistent with the

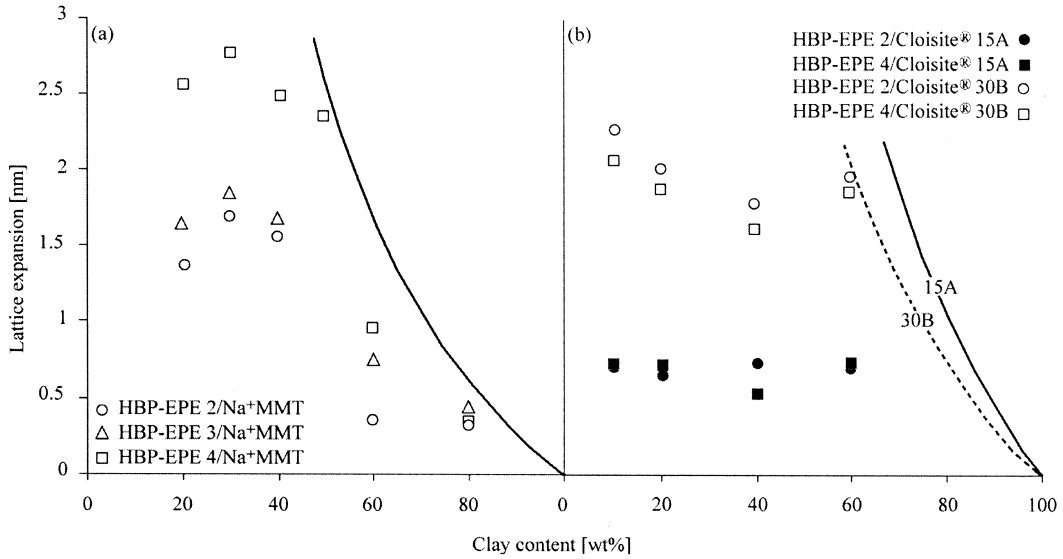

Fig. 5. Lattice expansion as a function of clay content in (a) HBP-EPE/Na^+MMT processed in water and (b) HBP-EPE mixed with different organically modified clays in THF.

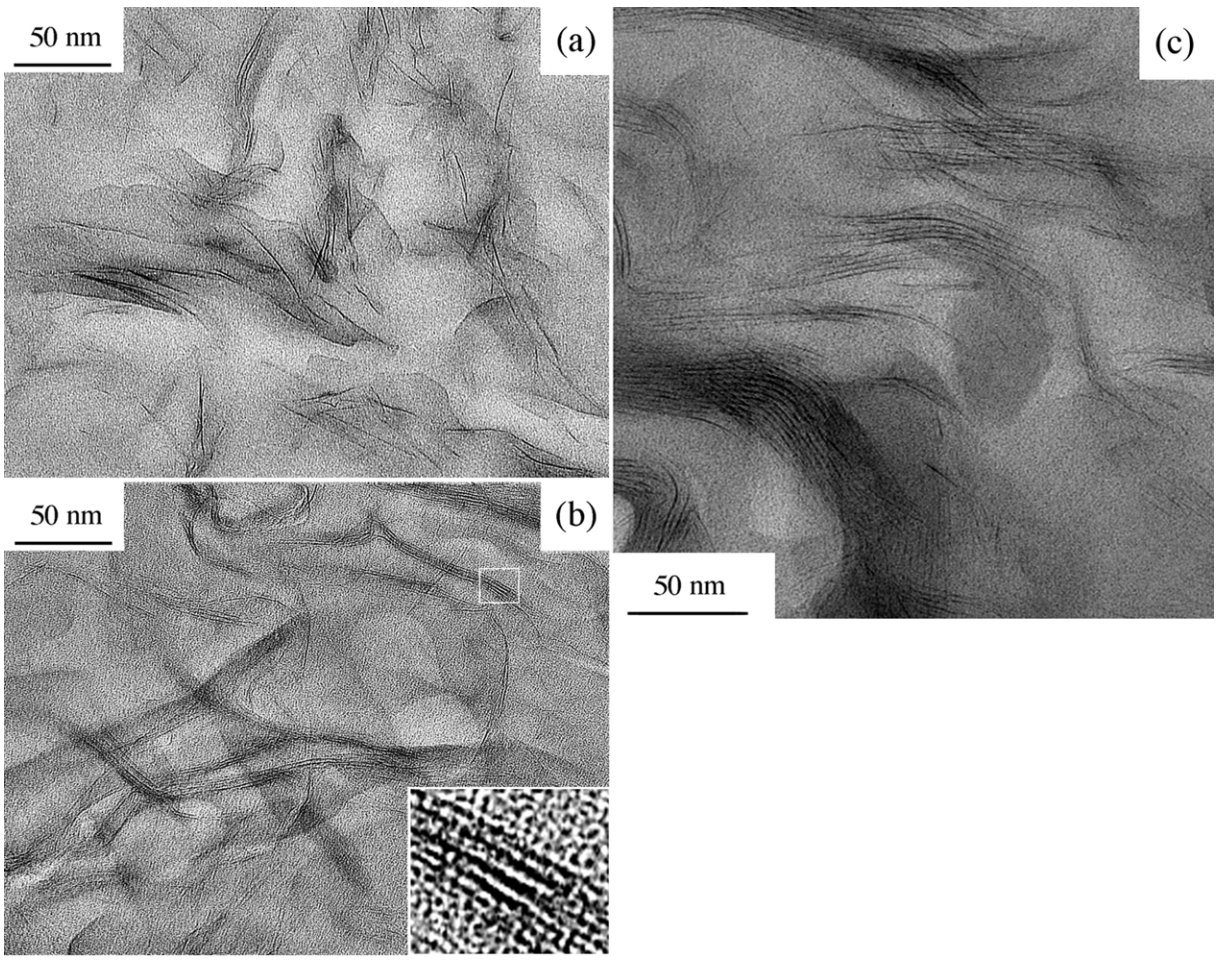

Fig. 6. TEM micrographs of thin sections of 2 pseudo-generation HBP-EPE/Na^{+}MMT processed in water: (a) 10 wt%; (b) 20 wt%, and (c) 2 pseudo-generation HBP-EPE/10 wt% Cloisite® 20A processed in THF.

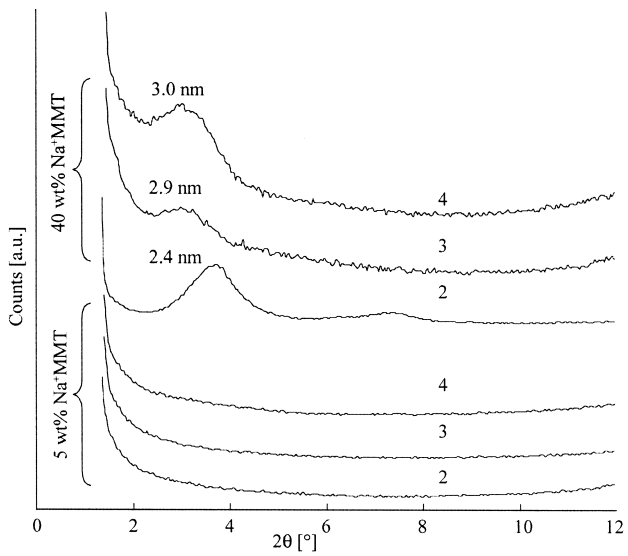

Fig. 7. WAXS spectra for different pseudo-generations of HBP-TMP/Na^{+}-MMT processed in water.

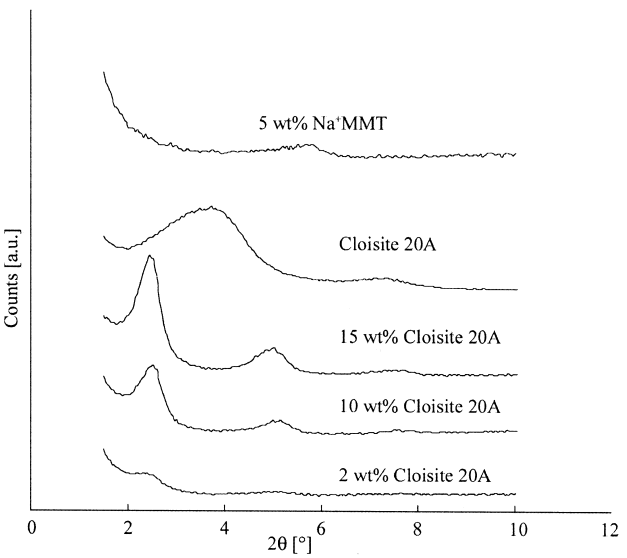

Fig. 8. WAXS spectra for polyoxetane/Cloisite® 20A processed in THF and polyoxetane/Na^{+}MMT processed in methanol.

observation of dendrimer intercalation with relative weak layer expansion under certain conditions (in the case of the dendrimers this cannot be accounted for by intercalation of a low molar mass fraction) [32]. There is also experimental evidence from atomic force microscopy (AFM) for flattened conformations when isolated polyester HBPs are absorbed onto mica substrates [33]. At high clay contents (above about 60 wt%), as shown in Fig. 5, where the HBP concentration is low, collapsed HBP conformations was assumed. These conformations may maximize the number of end-group interactions between an isolated dendrimer and the substrate, but they need not maximize the number of end-group interactions between the substrate in a many-chain system (a flattened conformation shields a relatively large surface area per molecule from further end-group attachment), and it has also been shown that the heights of concentrated absorbed layers are close to the unperturbed HBP molecular dimensions [33]. In Fig. 9 the layer expansion for HBP/Na^+MMT nanocomposites with intermediate clay contents has been plotted against M_n and the effective molecular diameter, $2r_g$, estimated from molecular dynamics simulations on isolated perfect dendrimer equivalents to each HBP at 700 °C using Cerius2 (Accelrys Inc.) with the Dreiding II forcefield (50 ps/0.001 time step, constant *PVT*, mean results for 4 different randomized seed conformations; similar results were obtained over the temperature range 300 to 1300 °C). Bearing in mind the effects of polydispersity, the agreement between the measured layer expansion and the estimates of the molecular sizes is consistent with the presence of a monolayer of un-collapsed HBP molecules at the surface of the silicate layers at intermediate Na^+MMT contents. It follows that the high degree of swelling of the Na^+MMT in aqueous dispersions containing relatively high concentrations of HBP permits dense coverage of the silicate layers by the HBP. For higher clay contents there was no longer sufficient HBP for these levels of layer expansion to be maintained in a homogeneous composite, particularly for the high pseudo-generation numbers.

3.1. Rheological properties of the HBP-based nanocomposites

Fig. 10 shows the results of rheological measurements on nanocomposites based on the 2 pseudo-generation HBP-EPE, which were selected for use in the polyurethanes. The nanocomposites were first preheated to 200 °C for one minute in order to erase aggregation effects associated with prior physical aging, which lead to poor reproducibility [30]. After preheating, the polyester HBPs showed Newtonian behavior in the melt. However, relatively small amounts of Na^+MMT (~0.7 wt%) were sufficient to induce significant increases in the viscosity over the whole range of shear rates investigated, and marked shear thinning (Fig. 10(a)). This is illustrated further in Fig. 11(a), which shows the magnitude of the complex viscosity, η^*, at 100 rad/s as a function of Na^+MMT content in the temperature range 120 to 200 °C. (Similar behavior was observed at other frequencies in the range investigated.) At each temperature, the viscosity showed a sharp increase at about 0.8 wt% Na^+MMT. This was therefore assumed to represent an approximate effective physical percolation threshold for the Na^+MMT in this type of measurement. Corresponding data for intercalated nanocomposites from 2 pseudo-generation HBP-EPE and Cloisite® 20A are also given in Figs. 10(b) and 11(b). The behavior of HBP-EPE/Cloisite® 20A composites was qualitatively similar to that of the exfoliated HBP-EPE/Na^+MMT nanocomposites. However, as shown in Fig. 11(b), η^* increased relatively slowly with Cloisite® 20A content, with roughly 10 times more clay being required to reach a given η^* than in 2 pseudo-generation HBP-EPE/Na^+MMT. This provides a further indication of

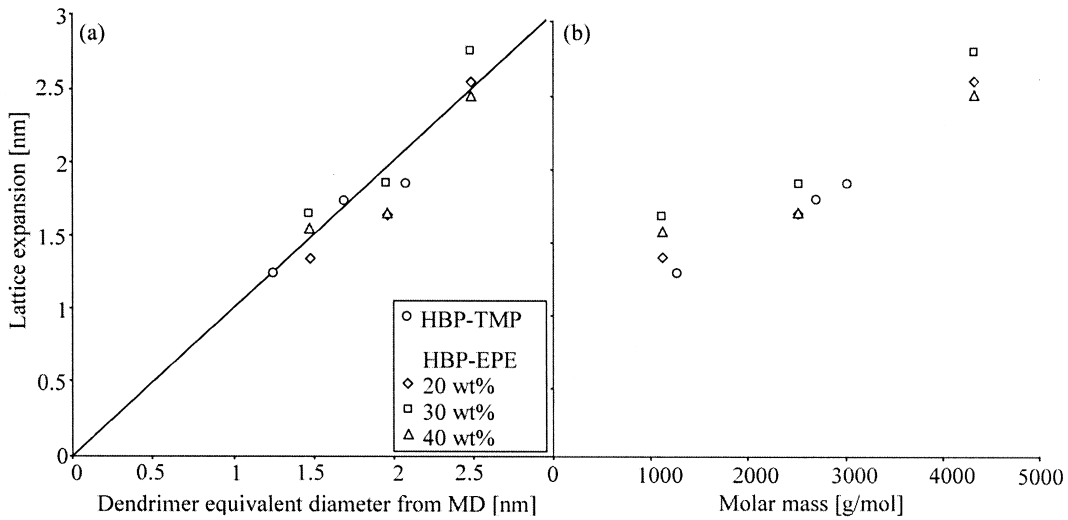

Fig. 9. Lattice expansion for different HBPs processed with Na^+MMT in water plotted against (a) $2r_g$, where r_g is the radius of gyration for the equivalent perfect dendrimer estimated from molecular dynamics simulations on isolated chains at 700 °C and (b) the measured M_n.

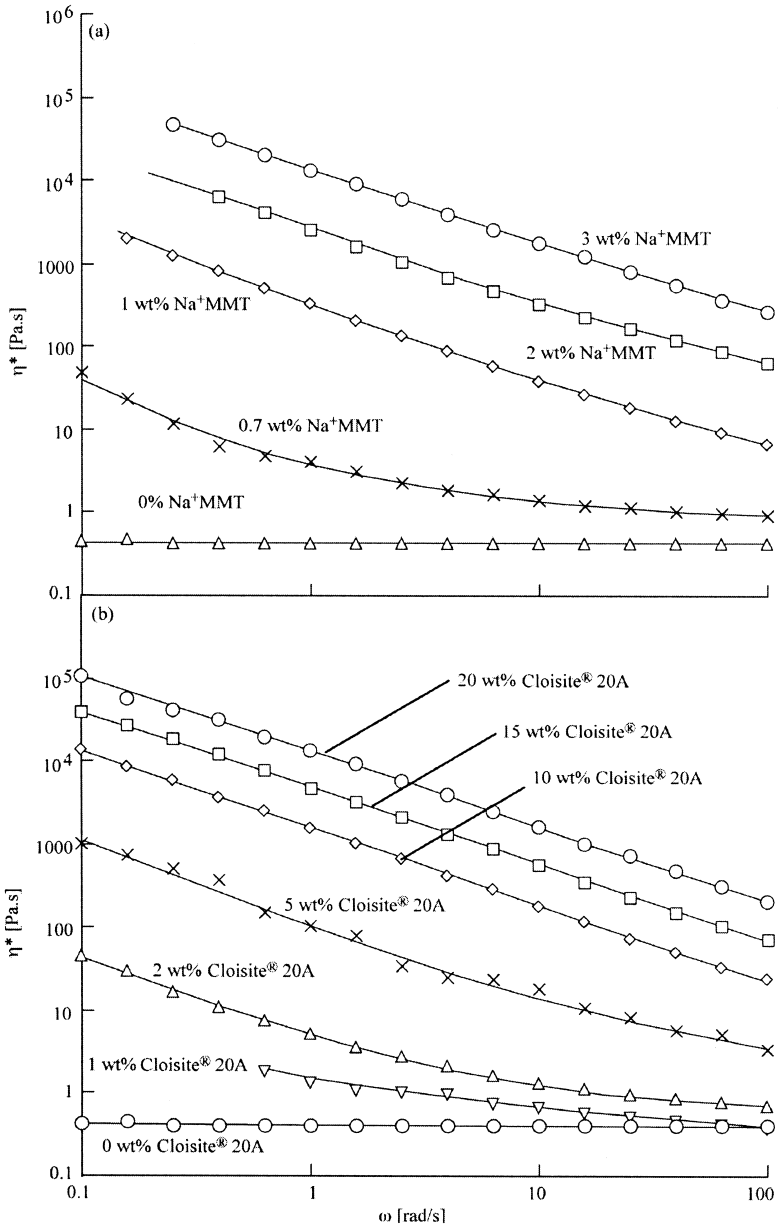

Fig. 10. η^* vs. ω at 150 °C for (a) 2 pseudo-generation HBP-EPE/Na^+MMT processed in water and (b) 2 pseudo-generation HBP-EPE/Cloisite® 20A processed in THF.

the high level of exfoliation of the Na^+MMT in the water processed composites.

Fig. 11(a) also reflects a decrease in the temperature sensitivity of η^* in HBP-EPE/Na^+MMT beyond the percolation threshold. Temperature sweeps at fixed frequency indicated Arrhenius dependence with an activation energy of about 75 kJ/mol for 2 pseudo-generation HBP-EPE and 100 kJ/mol for 4 pseudo-generation HBP-EPE, consistent with previous measurements [30]. However, the activation energy dropped to less than 15 kJ/mol in 2 pseudo-generation HBP-EPE/Na^+MMT contents beyond 1 wt%, and to less than 55 kJ/mol in 4 pseudo-generation HBP-EPE. These marked changes in rheological behavior were attributed to the effect of physical contacts between the filler particles rather than large changes in matrix mobility. In the exfoliated HBP-EPE/Na^+MMT nanocomposites, T_g generally remained independent of clay content within the experimental error of about ± 2.5 K. This also suggested limited molar mass degradation during processing, given that T_g is a strongly increasing function of molar mass in the range under consideration (Table 1). In the predominantly intercalated nanocomposites, T_g also varied little, but the transition was effectively suppressed at high clay contents. The only exception to these observations was 2 pseudo-generation HBP-EPE/Na^+MMT, which showed a small systematic increase in T_g from 381 to 391 °C as the MMT content was increased from 0 to 40 wt%. However, this was not considered sufficient to account for the orders of

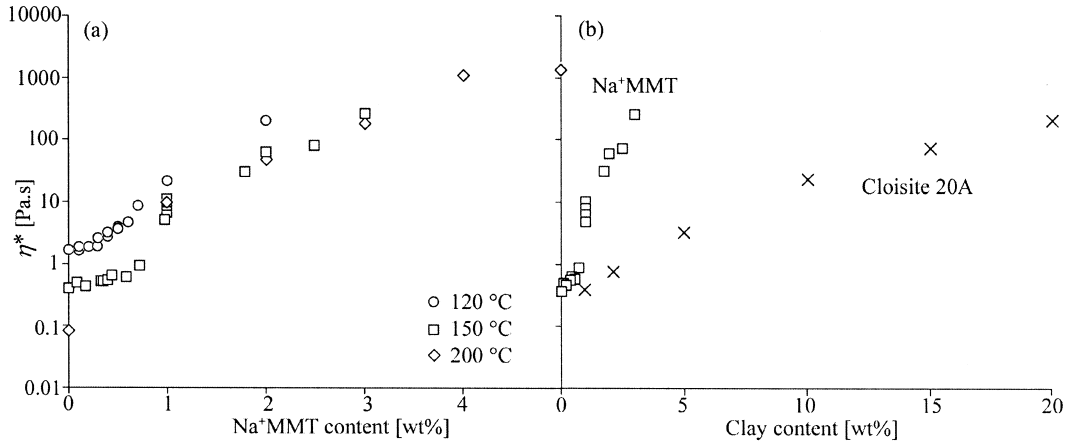

Fig. 11. η^* vs. ϕ for (a) 2 pseudo-generation HBP-EPE/Na^+MMT processed in water and tested at different temperatures and (b) 2 pseudo-generation HBP-EPE/Cloisite® 20A processed in THF tested at 150 °C.

magnitude increases in η^* on addition of a few wt% exfoliated Na^+MMT to the HBP (Fig. 11(a)). The rheological properties of HBP/clay nanocomposites will be further discussed in coming publication [34].

3.2. Polyurethanes

In conventional melt processing of polyurethane composites the inorganic filler is usually dispersed in a polyol prior to mixing with the diisocyanate hardener [15]. Efficient mechanical mixing may require not only a sufficiently low overall viscosity at the processing temperature, but also approximate viscosity matching between the different components, depending on the details of the mixing procedure. The rheological results described above therefore suggest that even a few wt% of highly exfoliated Na^+MMT in HBP-EPE could cause difficulties with processing at low shear rates with a low viscosity diisocyanate such as MDI, in spite of the relatively low melt viscosity of the unfilled 2 pseudo-generation HBP-EPE above its T_g.

To compensate, the low viscosity polyols PEG (300 g/mol) and ETMP, were used as reactive diluents for the HBP nanocomposites. Hand mixing the nanocomposites with the MDI at room temperature remained difficult in the presence of the low viscosity polyols, and the overall clay contents that could be introduced into the polyurethanes by this method was limited. However, even at low Na^+MMT contents, significant changes in mechanical properties were observed, reflecting an absence of Bragg peaks in the WAXS spectra and a relatively high degree of dispersion of the Na^+MMT subsequent to processing, as shown in corresponding TEM micrograph in Fig. 12(a). In polyurethanes produced from different amounts of exfoliated 2 pseudo-generation HBP/Na^+MMT (maximum 10 wt% Na^+MMT), the rubbery plateau modulus increased by up to 60% for an overall Na^+MMT content of 1.2 wt%, relative to that of the unfilled matrix of the same composition. The increase in modulus was far less marked for the same overall MMT content in the absence of HBP, as shown in Fig. 13(a), which gives data for formulations containing either PEG or ETMP, expressed as the reduced tensile modulus, $E'/E'(0$ wt% clay) as a function of Na^+MMT content. The corresponding TEM micrograph is shown in Fig. 12(b). Although the choice of polyol did not significantly influence the relative increases in modulus, the absolute values of the plateau modulus of polyurethanes prepared with ETMP (16 MPa) were somewhat higher than with PEG (12 MPa). On HBP addition, the α-transition temperature, T_α, increased from 40 to 50 °C in the polyurethanes prepared with PEG, but remained relatively constant at about 70 °C for those prepared with ETMP, although the plateau modulus increased by about 10% on addition of 10 wt% HBP. T_α was not significantly affected by the presence of the Na^+MMT in any of the nanocomposites.

Processing with a non-reactive solvent, such as THF, had the advantage that the amount of solvent used in processing was not dictated by the final composition. Moreover, HBP-EPE/Na^+MMT prepared in water and re-dispersed in THF remained exfoliated, regardless of the degree of dilution [18] (even though mixing HBP-EPE and Na^+MMT in THF resulted in weak intercalation and little exfoliation). Reaction with MDI and evaporation of the THF thus gave exfoliated polyurethanes. Results for the plateau modulus are shown in Fig. 13(b) for polyurethanes prepared in this way with up to 5 wt% Na^+MMT. The relative increase in modulus with Na^+MMT content in the polyurethanes containing exfoliated 2 pseudo-generation HBP-EPE/Na^+MMT was somewhat lower than for the melt mixed polyurethanes, but was again much higher than for polyurethanes prepared from HBP-EPE/Cloisite® 20A mixed in THF, which remained intercalated after cure, although d_{001} increased slightly from about 3.8 to 4 nm.

In tensile tests at room temperature, that is, below T_g, and at 4 mm/min, all the polyurethanes underwent brittle fracture at relatively low strains. As reported previously [18], the strength and high-strain stiffness in the exfoliated composites prepared using THF increased significantly with

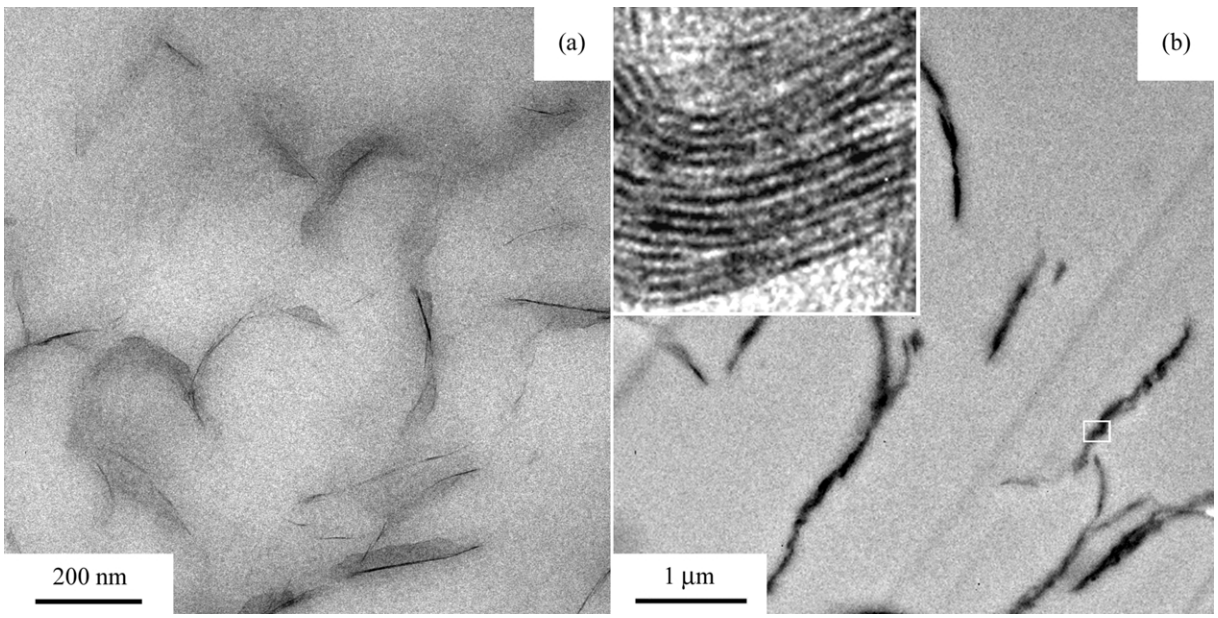

Fig. 12. TEM micrographs of (a) a 2 pseudo-generation HBP-EPE/polyol/MDI nanocomposite containing 1.2 wt% Na^+MMT and (b) a polyol/MDI nanocomposite containing 1.2 wt% Na^+MMT.

respect to that of the matrix, but there was a decrease in strain at break, and the Young's modulus was insensitive to clay content. The specimens that contained organically modified clay showed an increase in both strength and strain at break (cf. conventional polyurethane elastomers containing intercalated organically modified clays), but the increase in high strain stiffness was smaller than for the exfoliated composites.

4. Conclusions

Novel nanocomposites have been prepared from HBPs and various types of MMT. Dispersion of –OH functionalized polyester HBPs and unmodified Na^+MMT in water gave exfoliated nanocomposites at up to 20 wt% MMT after drying, and at intermediate MMT contents, the layer spacing in the resulting intercalated nanocomposites correlated closely with estimates of the molecular diameters of the different HBPs. Dispersions of the HBPs with various types of organically modified MMT in THF led to intercalation over the whole range of MMT contents, and the layer expansion in this case correlated with the polarity of the organic modifier rather than the size of the HBPs. Even though only limited amounts of exfoliated HBP/MMT nanocomposites could be introduced into polyurethane formulations by the simple mixing procedures employed here, large increases in the plateau modulus at low Na^+MMT loadings were observed.

Acknowledgements

We would like to thank the Swiss CTI-Top Nano 21

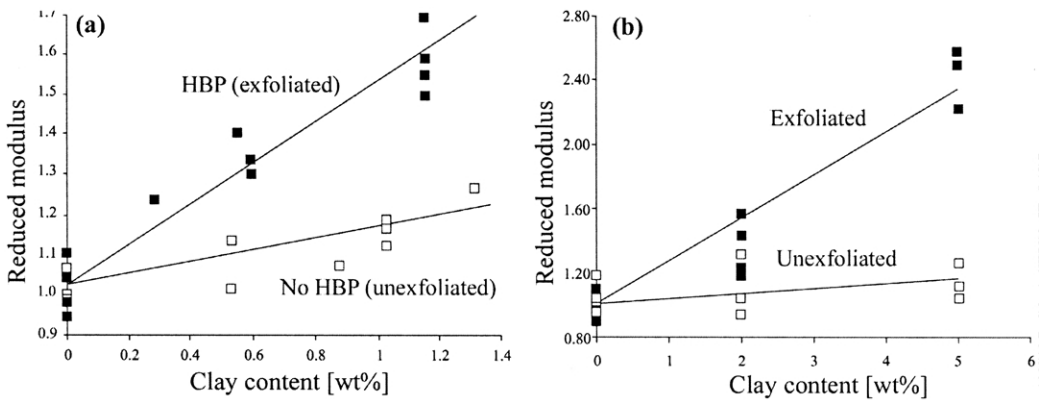

Fig. 13. The rubbery plateau modulus normalized with respect to the plateau modulus for $\phi = 0$ in: (a) 2 pseudo-generation HBP-EPE/polyol/MDI/Na^+MMT composites (filled squares) and polyol/MDI/Na^+MMT composites (open squares) at 120 °C; (b) exfoliated 2 pseudo-generation HBP-EPE/Na^+MMT dispersed with MDI in THF (filled squares) and the same formulation containing unexfoliated Cloisite® 20A (open squares) at 160 °C.

initiative and Dow Europe for their financial support, and the Centre Interdisciplinaire de Microscopie Electronique (CIME).

References

[1] Jiankun L, Yucai K, Zongneng Q, Xiao-Su Y. J Polym Sci Part B: Polym Phys 2001;39:115–20.
[2] Lan T, Kaviratna D, Pinnavaia TJ. J Phys Chem Solids 1996;57(6-8): 1005–10.
[3] Wang MS, Pinnavaia TJ. Chem Mater 1994;6(4):468–74.
[4] Wang Z, Lan T, Pinnavaia TJ. Chem Mater 1996;8(9):2200.
[5] Wang Z, Pinnavaia TJ. Chem Mater 1998;10(7):1820–6.
[6] Messersmith PB, Giannelis EP. Chem Mater 1994;6(10):1719–25.
[7] Yasmin A, Abot JL, Daniel IM. Scripta Mater 2003;49(1):81–6.
[8] Zilg C, Thomann R, Mulhaupt R, Finter J. Adv Mater 1999;11(1): 49–52.
[9] Ma J, Zhang S, Qi Z. J Appl Polym Sci 2001;82:1444.
[10] Tien YI, Wei KH. Polymer 2001;42(7):3213–21.
[11] Yao KJ, Song M, Hourston DJ, Luo DZ. Polymer 2002;43(3): 1017–20.
[12] Chen TK, Tien YI, Wei KH. Polymer 2000;41(4):1345–53.
[13] Wang Z, Pinnavaia TJ. Chem Mater 1998;10(12):3769–71.
[14] Zhang XY, Klein J, Sheiko SS, Muzafarov AM. Langmuir 2000; 16(8):3893–901.
[15] Woods G. The ICI polyurethanes book. Chichester: ICI Polyurethanes and Wiley & Sons; 1990.
[16] Torro-Palau AM, Fernandez-Garcia JC, Orgiles-Barcelo AC, Martin-Martinez JM. Int J Adhes Adhes 2001;21(1):1–9.
[17] Ogata N, Kawakage S, Ogihara T. J Appl Polym Sci 1997;66(3): 573–81.
[18] Plummer CJG, Garamszegi L, Leterrier Y, Rodlert M, Månson J-AE. Chem Mater 2002;14(2):486–8.
[19] Malmstrom E, Johansson M, Hult A. Macromolecules 1995;28(5): 1698–703.
[20] Hult A, Johansson M, Malmström E. Hyperbranched polymers. In: Roovers J, Roovers J, editors. Branched polymers II. Advances in polymer science, vol. 143. Berlin: Springer; 1999.
[21] Mezzenga R, Boogh L, Månson J-AE. Compos Sci Technol 2001; 61(5):787–95.
[22] Plummer CJG, Mezzenga R, Boogh L, Månson J-AE. Polym Engng Sci 2001;41(1):43–52.
[23] Mezzenga R, Plummer CJG, Boogh L, Månson J-AE. Polymer 2001; 42(1):305–17.
[24] Boogh L, Pettersson B, Månson J-AE. Polymer 1999;40(9):2249–61.
[25] Holter D, Burgath A, Frey H. Acta Polym 1997;48(1–2):30–5.
[26] Hawker CJ, Lee R, Frechet JMJ. J Am Chem Soc 1991;113(12): 4583–8.
[27] Magnusson H, Malmstrom E, Hult A. Macromol Rapid Commun 1999;20(8):453–7.
[28] Garamszegi L, Plummer CJG, Rodlert M, Månson J-AE. In preparation.
[29] Garamszegi L, Nguyen TQ, Plummer CJG, Månson J-AE. J Liquid Chromatogr 2003;26(2):203–26.
[30] Plummer CJG, Luciani A, Nguyen TQ, Garamszegi L, Rodlert M, Månson J-AE. Polym Bull 2002;49(1):77–84.
[31] http://www.scprod.com/.
[32] Plummer CJG, Månson J-AE. 14th International Conference on Composite Materials (ICCM 14), San Diego; July 2003.
[33] Tsukruk VV. Adv Mater 1998;10(3):253–7.
[34] Rodlert M, Plummer CJG, Leterrier Y, Månson J-AE. J Rheol. Submitted for publication.